

Switchable/Tunable Dual-Band BPF for Bluetooth and 5G NR Applications

Areeg F. Hussein^{1,*}, Malik Jasim Farhan¹, and Jawad K. Ali²

¹Electrical Engineering Department, College of Engineering, Mustansiriyah University, Baghdad, Iraq

²Communication Engineering Department, University of Technology, Baghdad, Iraq

ABSTRACT: This article presents a dual-band switchable and tunable band-pass filter for Bluetooth and 5G NR applications. The filter functions at 2.41 GHz for Bluetooth and 3.55 GHz for 5G, utilizing independent switching and tuning methods facilitated by PIN and varactor diodes. The suggested design exhibits compact dimensions of $0.177\lambda_g \times 0.096\lambda_g$, a minimal insertion loss of 0.35 dB, and a substantial return loss of 30 dB. Advanced design methodologies, including defective ground structures (DGS) and Eigenmode analysis, were utilized to attain precise selectivity and exceptional out-of-band rejection. The engineered filter demonstrates superior performance, with outcomes closely aligning with models, and guarantees little interference with suppression up to 10 GHz. The tuning mechanism provides versatility by independently modifying the operating frequencies of the second band, rendering the design very flexible for dynamic wireless communication settings. This study emphasizes a robust and effective answer for contemporary mobile communication systems.

1. INTRODUCTION

Mobile communication systems rely on band-pass filters to let signals within a specified frequency range flow through while rejecting signals outside this range. For mobile networks to guarantee efficient and noiseless communication, selective frequency management is essential [1, 2]. Many short-range wireless communication technologies, including Wi-Fi and Bluetooth, operate in the 2.4 GHz band, a component of the industrial, scientific, and medical (ISM) radio band [3].

Its interoperability with many devices and its capacity to offer dependable access in heavily crowded places make it a favorite. Likewise, more recent 5G rollouts employ 3.5 GHz range, the Citizens Broadband Radio Service (CBRS) spectrum. Optimal for improving mobile broadband services, fixed wireless access, and meeting the increasing need for high-speed data transmission in urban and suburban areas, this band balances coverage and capacity [4, 5].

To simultaneously accomplish narrow and wide passbands, [6] introduces a unique dual-band band-pass filter developed with a stepped-impedance ring-loaded resonator (SIRLR). The filter has a 2.4 GHz tight passband and a 3 to 5 GHz wide passband, which has minimal insertion losses. To increase the band rejection level to 25 dB, rectangular stub-loaded resonators (RSLRs) are used to broaden the stopband from 5 to 20 GHz.

In [7], two dual-band balanced microstrip band-pass filters (BPFs) use open stub-loaded resonators (OSLRs) and short stub-loaded resonators (SSLRs). The filters are intended to function at 1.9/2.5 GHz and 2.4/3.5 GHz, respectively,

center frequencies. Modifying the resonator lengths allows the differential-mode (DM) passbands to be controlled quasi-independently. A stepped impedance microstrip line etched with an interdigital coupling line improves selectivity by increasing the coupling between resonators and creating more transmission zeros (TZs).

In [8], a tunable dual-band balanced filter, including a significant stopband and transmission zeros, employs a pair of electromagnetically connected stepped impedance resonators (SIRs). The coupling space of the feeding lines and the ratio of the electric and magnetic coupling coefficients of the SIR pair may be manipulated to control four transmission zeros centered on the two operating bands. The filter demonstrated a broad and significant stopband, surpassing 40 dB attenuation, along with good common mode suppression, designed and assessed at 1.75 GHz and 3.64 GHz,

In [9], the authors introduced a new dual-band in-phase filtering power divider (FPD) based on terminated coupled lines. The design equations were formulated, and the prototype FPD was simulated, manufactured, and evaluated. The FPD operated at 4.11 GHz and 6.56 GHz frequencies, which is well suited for contemporary wireless multi-band communication systems.

The design of a miniature microstrip band-pass filter using square defective microstrip structure (DMS) slots was presented in [10], and the filter was constructed using two identical rectangular resonators realized by microstrip technology. The DMS was applied to the filter by etching grooves in the resonator, enhancing effective inductance and capacitance. In [2], the authors presented a compact dual-band BPF design employing two folded $\lambda_g/2$ resonator lines with 3.5 GHz and 5.45 GHz

* Corresponding author: Areeg F. Hussein (areeg-fadhil@uomustansiriyah.edu.iq).

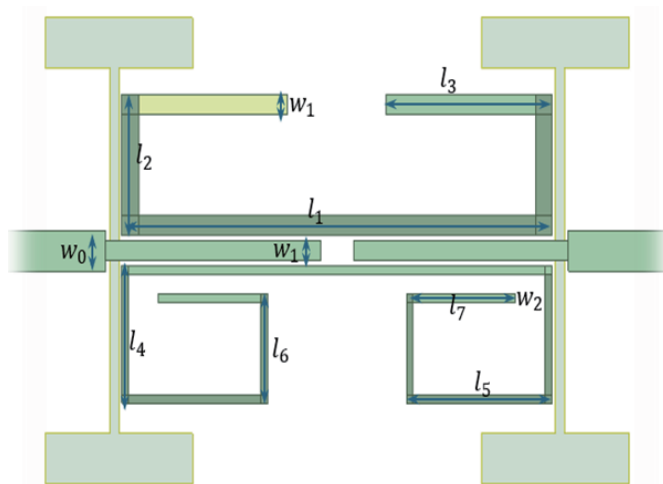


FIGURE 1. The proposed filter layout.

operating frequencies. The design incorporates four transmission zeros to ensure separated bands and enhance performance.

The authors in [11] presented BPFs employing mixed Eighth-mode Substrate Integrated Waveguide (EMSIW) and microstrip line (MSL) resonators in both single and dual bands. The mix of EMSIW and MSL demonstrated a compact circuit size, a modest-quality factor, and a flexible design topology. In [12], interdigit resonators (HPF & LPF) were combined with stub-loaded resonators to provide a notch to present a tunable switchable BPF. The design was complicated with bad insertion and return losses (3.9 dB–10 dB).

The authors in [13] introduced a band-pass filter that can be adjusted to a band-stop filter using a split ring resonator (SRR) with stepped impedance resonators. Another SRR was proposed by [3], where a band-pass filter may be designed with adjustable frequency change according to the glucose level in the blood. In [14], the authors presented a reconfigurable band-pass to band-stop filters using a PIN diode that connects or disconnects a $\lambda_g/4$ stub resonator to a ring resonator.

The researchers in [15] presented a miniature dual/single-band adjustable band-pass filter (BPF) fabricated from FR4 epoxy material and intentionally built for adjustability using HSCH 3486 PIN diodes. The design, including semicircular chambers and interconnecting feeding lines, was simulated with HFSSv13 and fabricated by chemical etching. The filter demonstrated resonance at frequencies of 3.7 and 5.2 GHz, with an impedance bandwidth of 2.4 GHz. Upon deactivating the PIN diode, the filter showed resonance at a frequency of 6.7 GHz, meeting the criteria for X-band satellite communication applications.

In [12], a fully adjustable band-pass filter was introduced with an extensive bandwidth tuning range. It may also alternate between single and dual-band operations. The design included a tunable low-pass filter, a tunable high-pass filter, and a switchable notch filter arranged in a cascade configuration. The center frequency and bandwidth of the band-pass filter may be altered by adjusting the cutoff frequencies of the low-pass and high-pass filters. The BPF demonstrated remarkable adaptability, operating in single passband, dual passbands,

and all-off modes. The bandwidth was modified between 0.25 and 2.69 GHz, while the center frequency was modified between 2.9 and 4.6 GHz. The absolute bandwidth remained fixed at 1 GHz. The BPF exhibited elevated out-of-band rejection levels across all modes, making it suitable for carrier aggregation applications. The measured results validated the design, demonstrating exceptional performance with little insertion loss and substantial return loss, exhibiting a strong correlation with simulated outcomes.

This paper presents a switchable/tunable dual band-pass filter used in mobile communications. The first band, centered at 2.41 GHz, used in Bluetooth applications, can be switched on or off according to user demand, and the second band operates at 3.55 GHz, the new radio band in the 5G network. Fig. 1 presents the proposed filter layout.

2. FILTER DESIGN AND FABRICATION

This section will address the proposed filter design procedures, analysis, simulation, and fabrication.

2.1. Filter Design and Analysis

The proposed dual-band filter is defined by the following parameters: a filter order of 1, center frequencies of 2.4 GHz and 3.55 GHz, fractional bandwidths of 7.9% and 11.83%, and a return loss (RL) of 30 dB. The physical lengths l of the resonators in Fig. 1 are determined using the following equations [16]:

$$\lambda_g = \frac{300}{f(\text{GHz})\sqrt{\epsilon_{re}}} \quad (1)$$

$$\epsilon_{re} = \frac{\epsilon_r + 1}{2} + \frac{\epsilon_r - 1}{2} \left\{ \left(1 + 12 \frac{h}{w} \right)^{-0.5} + 0.04 \left(1 - \frac{w}{h} \right)^2 \right\} \quad (2)$$

where λ_g is the guided wavelength at a center frequency, h the substrate thickness of 0.508 mm, ϵ_r the dielectric constant of 3.55, and w the conductor width. $l = \lambda_g/3$. The Eigenmode analysis technique builds and optimizes filter resonators to resonate at the designated operating frequencies.

The dimensions of each resonator were adjusted until the resonance frequencies were achieved, as presented in Fig. 2. Table 1 shows the eigenmodes for each resonator. Table 2 shows the dimensions of the final layout of the dual band-pass filter.

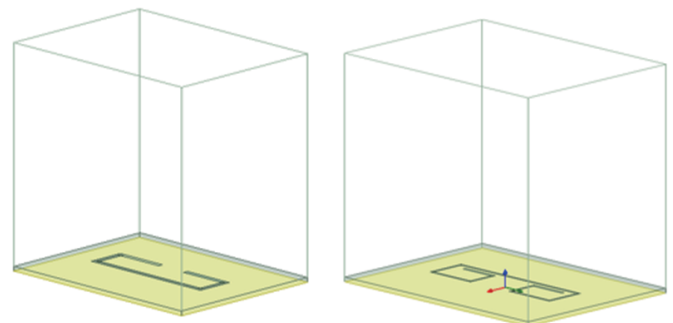


FIGURE 2. Eigenmodes analysis.

TABLE 1. Eigenmode solution for the resonator.

Band	Eigenmode	Frequency (GHz)
Band 1	Mode 1	2.40299 + $j0.00273832$
	Mode 2	4.66581 + $j0.00503860$
	Mode 3	7.08694 + $j0.00774342$
Band 2	Mode 1	3.13292 + $j0.00369580$
	Mode 2	6.65862 + $j0.00772923$
	Mode 3	8.25317 + $j3.31850e - 06$

TABLE 2. The final dimensions of the filter.

l1	l2	l3	l4	l5	l6	l7
13	3.5	5	3.4	4.4	2.7	3.3
w0	w1	w2	ϵ_r	h	Tangent loss	
1	0.5	0.2	3.55	0.508	0.0022	

The equivalent circuit model of the upper band of the filter is presented in Fig. 3. The response of the LC circuit for the upper band is presented in Fig. 4, while the equivalent circuit of the lower band is presented in Fig. 5, and its response is presented in Fig. 6.

LC values of the two bands are presented in Table 3.

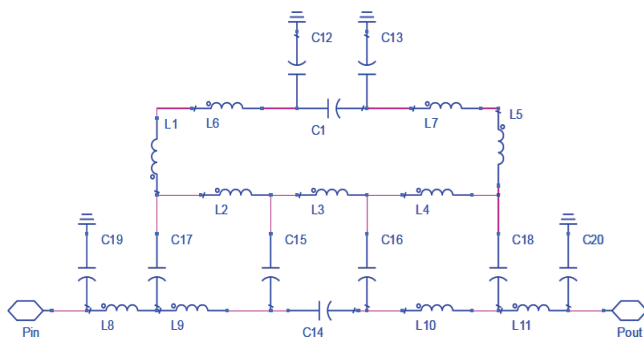


FIGURE 3. Equivalent circuit of the upper band.

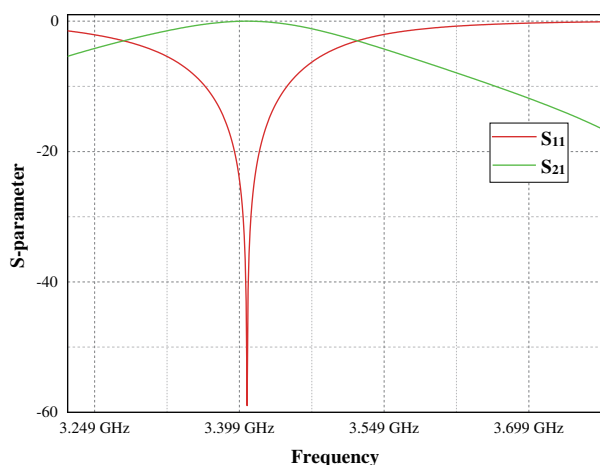


FIGURE 4. LC circuit S-parameter of the upper band.

2.2. Simulation and Fabrication of the Filter

The outcome of the filter after constructing it, along with the input/output port, is shown in Fig. 7. There are harmonics at 4.7 and 7.3 GHz, as can be seen.

A defected ground structure technique was applied to eliminate these harmonics, yielding the structure in Fig. 1 with a compact size of $(0.177\lambda_g \times 0.096\lambda_g)$ and the response shown in Fig. 8.

The resonance frequency for band 1 is 2.4 GHz at $S_{11} -29.5$ dB, $S_{21} -0.35$ dB, and sharp selectivity with a transmission zero at 2.8 GHz that has S_{21} of -35 dB, and the resonance frequency for band 2 is 3.5 GHz at $S_{11} -26.7$ dB, $S_{21} -0.4$ dB, and sharp selectivity with a transmission zero at 4 GHz that has S_{21} of -22.5 dB. The band suppression is up to 10 GHz. The final filter was fabricated, and the resonance frequencies of the filters agreed with the simulated ones except for a slight difference in the S_{11} and S_{21} parameters, as presented in Figs. 9 and 10.

3. TUNING AND SWITCHING MECHANISM OF THE FILTER

Tuning and switching the microstrip band-pass filters is commonly applied using varactor and PIN diodes, where the center frequency would be adjusted according to their states. The electric field distributions on the dual band-pass filter are presented in Figs. 11(a) and (b) to define the locations for the tuning varactor and switching PIN diode.

Switching the first band by putting the PIN diode in the red position where it can be turned on and off; hence, it operates as a Bluetooth band. The off-state appears in Fig. 12, which shows that the second band has not been affected since the two bands are independent.

Tuning band 2 using a varactor diode (varicap) will act as variable capacitance when it is reverse bias. The capacitor value of the varicap is calculated using Equation (3) from Chapter 13 in [16]:

$$C_l = \frac{Y_a C \cot \Theta_o}{2\pi f_o} \quad (3)$$

where Y_a is the characteristic admittance of the resonator, Θ_o the electrical length, and f_o the center frequency. The varicap has been connected in the gap of the open ring; the tuning circuit is presented in Fig. 13.

4. TUNING RESULTS AND DISCUSSION

The present study presents the fruitful design of a fully independent dual-band band-pass filter by showing that the two pass-band frequencies may be adjusted independently, as shown in Fig. 12. The change in the values of C in Fig. 13 presented a shift in the center frequency of band 2; Fig. 14(a) shows the S_{11} results.

At $C = 0.01$ pf, the center frequency shifted to 3.4 GHz with $S_{11} -35$ dB; at $C = 0.03$ pf, the center frequency shifted to 3.2 GHz with $S_{11} -33$ dB; at $C = 0.05$ pf, the center frequency shifted to 3.1 GHz with $S_{11} -34.9$ dB; at $C = 0.07$ pf, the center frequency shifted to 3 GHz with $S_{11} -30.3$ dB; at

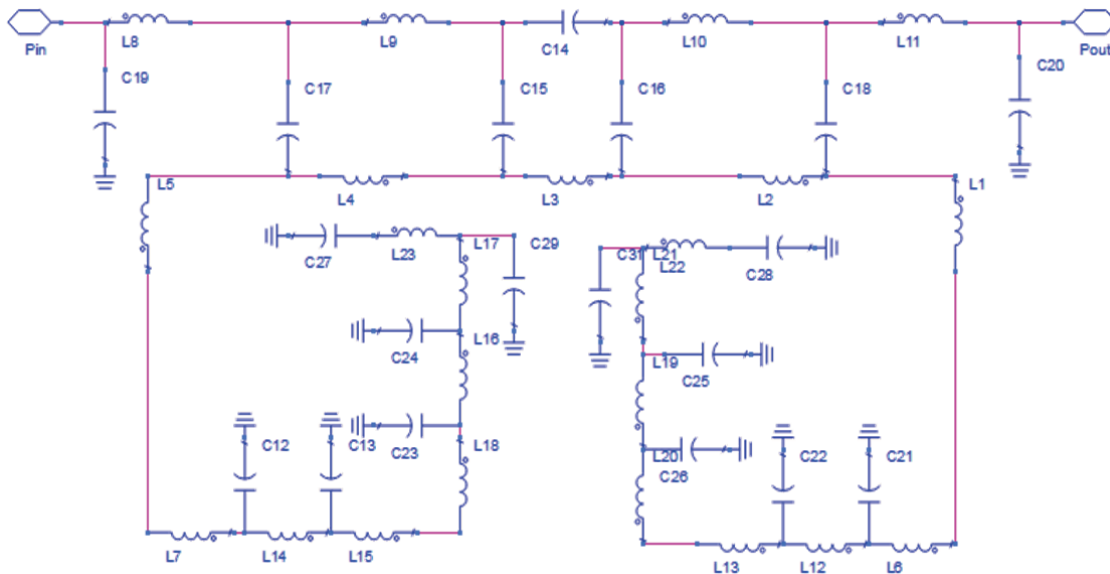


FIGURE 5. Equivalent circuit of the lower band.

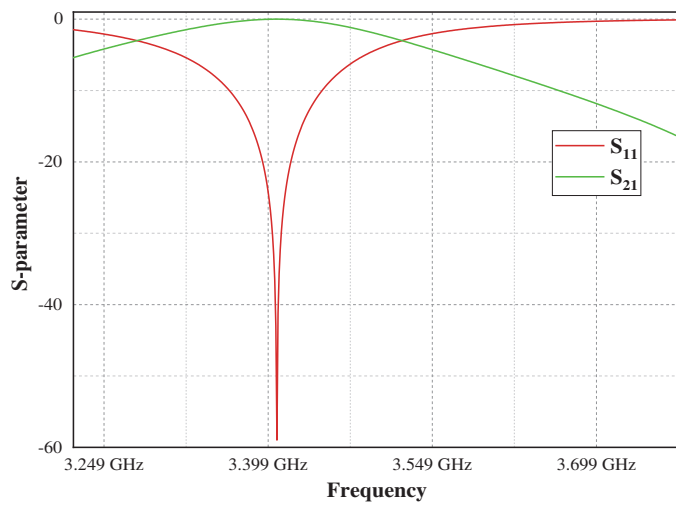


FIGURE 6. LC circuit S -parameter of the lower band.

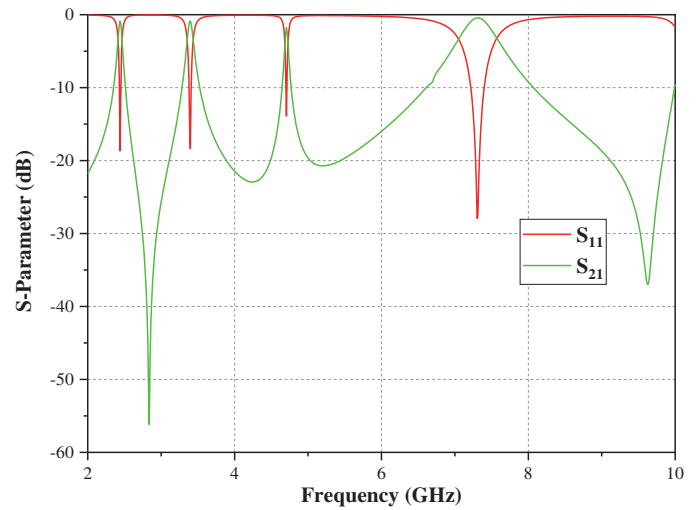


FIGURE 7. Filter response without DGS.

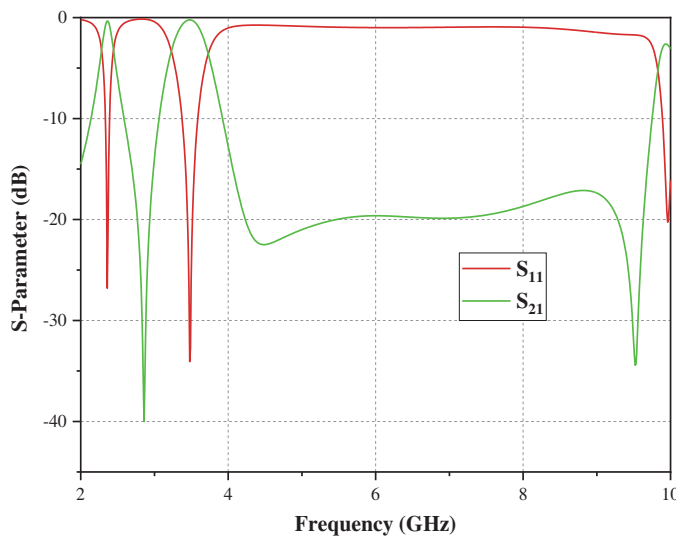


FIGURE 8. Filter response with DGS.

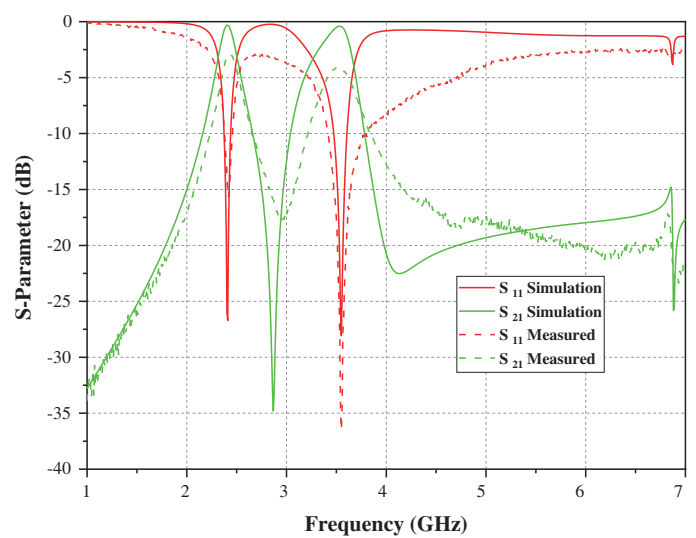


FIGURE 9. Comparison of simulated and fabricated results.

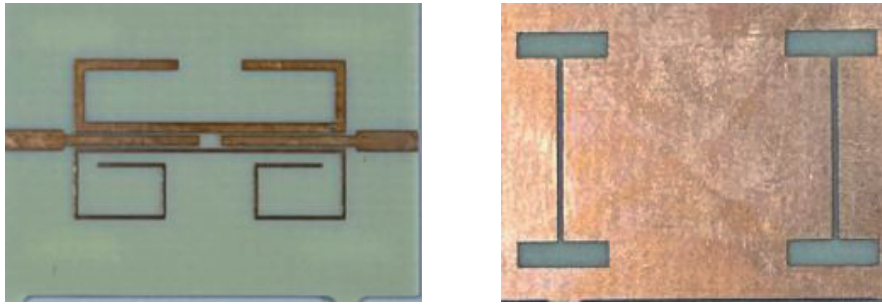


FIGURE 10. The fabricated dual-band filter.

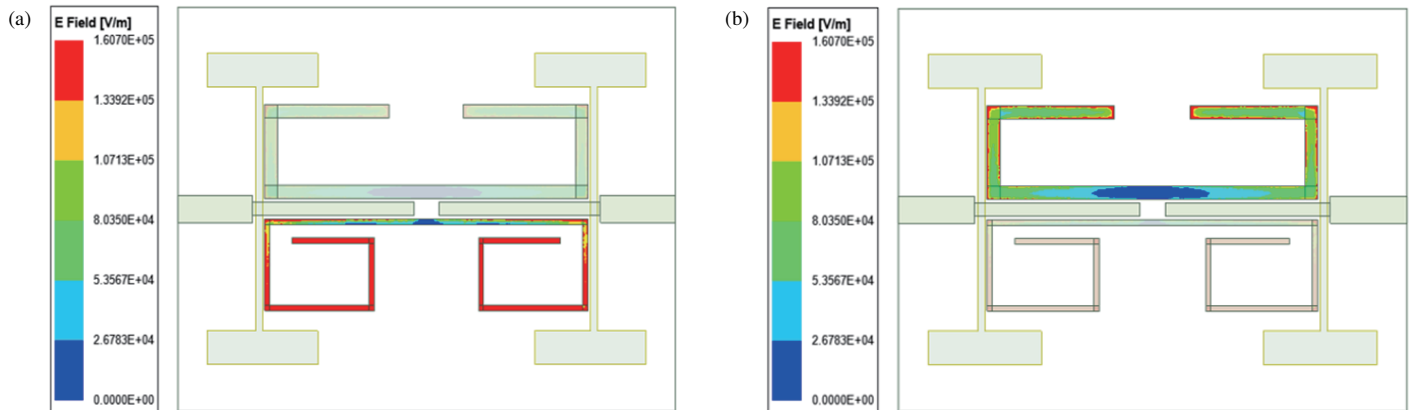


FIGURE 11. Electric field distribution (a) band 1, (b) band 2.

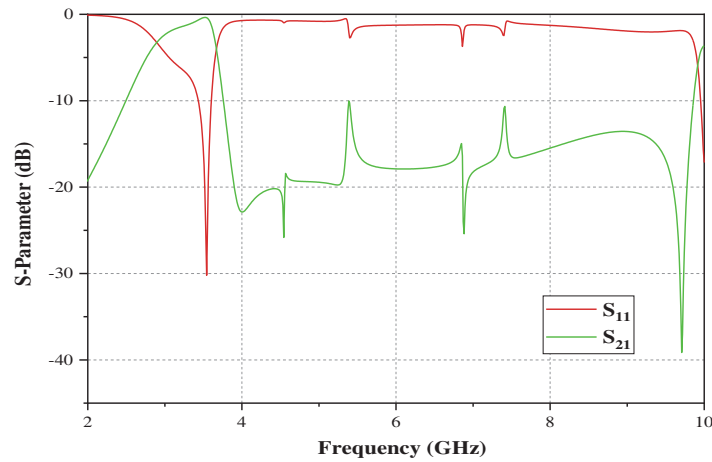


FIGURE 12. Switching band 1 off.

$C = 0.09$ pf, the center frequency shifted to 2.9 GHz with $S_{11} -22.3$ dB. The band suppression decreased slightly to 9 GHz as seen in Fig. 10(b), and band 1 is unaffected. Fig. 15 shows the S_{21} results. At $C = 0.01$ pf, the center frequency shifted to 3.4 GHz with $S_{21} -0.29$ dB.

At $C = 0.03$ pf, the center frequency shifted to 3.2 GHz with $S_{21} -0.25$ dB; at $C = 0.05$ pf, the center frequency shifted to 3.1 GHz with $S_{21} -0.27$ dB; at $C = 0.07$ pf, the center fre-

quency shifted to 3 GHz with $S_{21} -0.35$ dB; at $C = 0.09$ pf, the center frequency shifted to 2.9 GHz with $S_{11} -0.54$ dB.

Table 4 compares this work with the previous work, where the proposed antenna provides an expanded operational range, reduced insertion loss, enhanced return loss, compact dimensions, and improved rejection performance, rendering it a preferable option relative to alternatives.

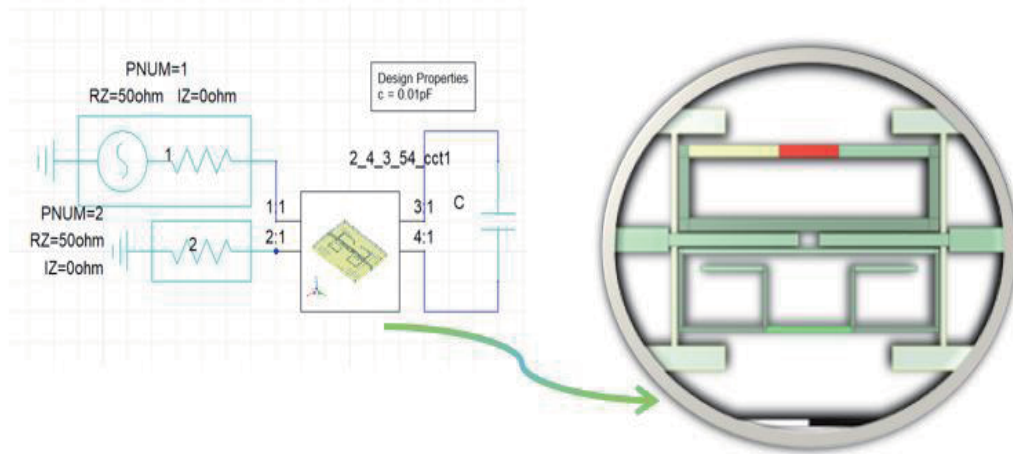


FIGURE 13. Tuning circuit of band 2 with band 1 on.

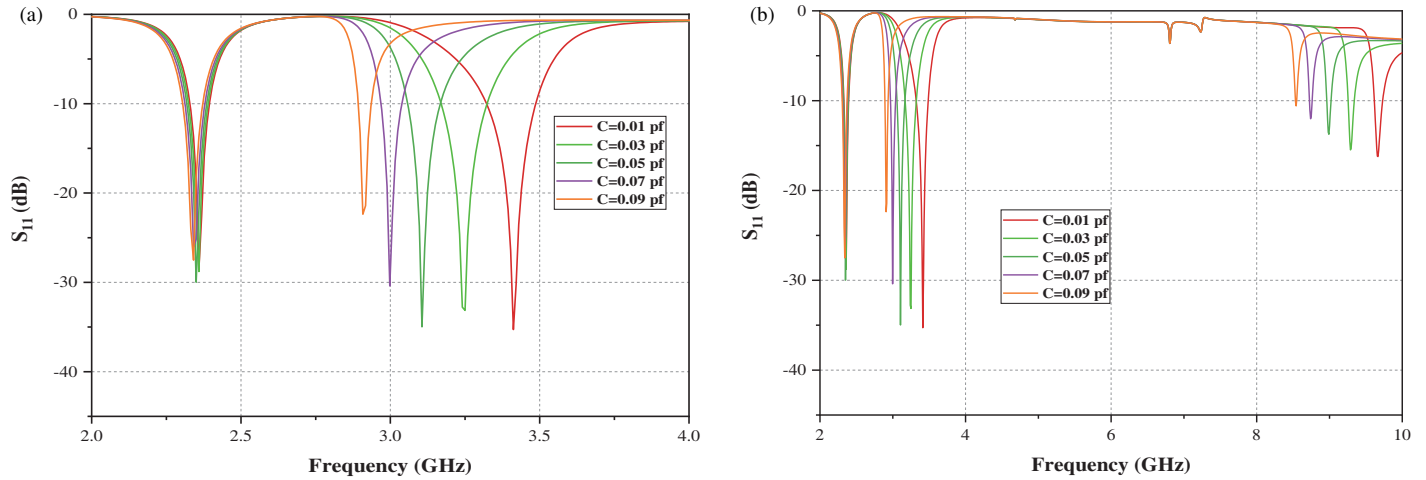


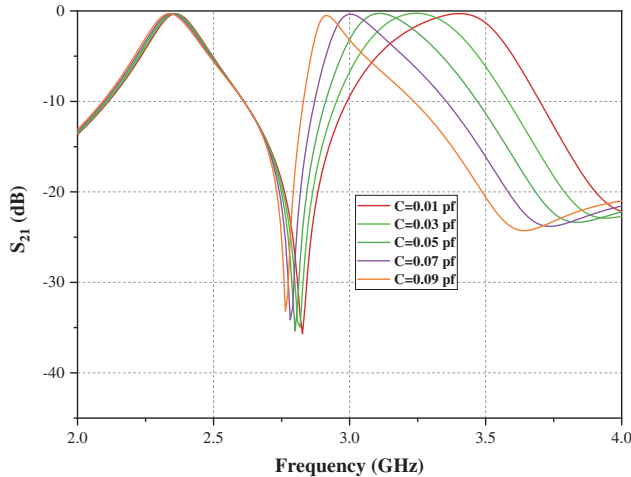
FIGURE 14. S_{11} of tuning band 2.

TABLE 3. LC values of the upper band.

Band 1	Value		Band 2	Value	
L (nH)	$L1$	0.974	L (nH)	$L1 = L5$	1.458
	$L2 = L4$	0.55		$L2 = L4 = L21$	1.35
	$L3$	0.509		$L3$	1.438
	$L5 = L7$	0.5		$L6 = L7$	0.854
				$L14 = L12 = L22$	0.57
C (pf)	$C1 = C14$	0.5	C (pf)	$C14 = C15 = C16 = C17 = C18 = C19$	0.58
	$C12$	1.499		$C20$	1.196
	$C13$	0.507		$C12 = C13 = C21 = C22$	1.47
	$C17 = C18$	1.48		$C23 = C26 = C31$	0.854
	$C15 = C16$	1.125		$C24 = C25 = C27 = C28$	0.585
	$C19 = C20$	1.495		$C29$	1.07

TABLE 4. Comparison with previous work.

Ref.	Frequency range (GHz)	Insertion loss (dB)	Return loss (dB)	Dimensions $\lambda_g * \lambda_g$	Rejection level (dB)
[17]	0.56–0.98	3.9	> 20	0.27×0.09	N.M
[12]	2.9–4.6	3.8	> 10	0.18×0.69	30
[18]	0.8–1.95	5.2	> 11.5	0.1×0.3	20
[19]	10.2–15.7	3.9	> 10	0.74×2.2	25
Props.	2.4–3.5	3.5	> 25	0.17×0.09	35

**FIGURE 15.** S_{21} of the tuning circuit of band 2.

5. CONCLUSION

The proposed dual-band band-pass filter, functioning at 2.41 GHz for Bluetooth and 3.55 GHz for 5G, exhibited efficient frequency management, compact size, and selectivity. This work has established that tuning mechanisms, including PIN and varactor diodes, permit independent control of two frequency bands, underlining flexibility for various mobile communication applications. The fabrication results agreed with simulations, demonstrating robust performance with minimal insertion loss differences and efficient out-of-band rejection. The developed filter presents a viable option for modern wireless communication systems, offering flexible performance and practical spectrum usage.

ACKNOWLEDGEMENT

The authors thank Dr. Hussam H. Ali Al-Saedi, Ameer Basheer, and Hussein Al-Jeshami for providing the microwave measurement infrastructure for the experimental setup and supporting the fabrication and measurements. The authors thank Mustansiriya University, College of Engineering (www.uomustansiriya.edu.iq) Baghdad-Iraq for its support in the present work.

REFERENCES

- [1] Patel, S., V. Shah, and M. Kansara, "Comparative Study of 2G, 3G and 4G," *International Journal of Scientific Research in Computer Science, Engineering and Information Technology*, Vol. 3, No. 3, 1962–1964, 2018.
- [2] Khani, H. I. and A. S. Ezzulddin, "Design of a compact dual-band BPF for 5G mobile communications using folded $\lambda_g/2$ -line resonators," in *2022 Muthanna International Conference on Engineering Science and Technology (MICEST)*, 71–76, Samawah, Iraq, Mar. 2022.
- [3] Alsultani, A. B., O. S. Alkhafaf, A. Szlavecz, J. G. Chase, and B. Benyó, "Design of high sensitivity split ring resonator sensor for invasive blood glucose monitoring," *IFAC-Papers On-line*, Vol. 58, No. 24, 303–308, 2024.
- [4] Basheer, A., H. Abdulhussein, H. Al-Saedi, and J. K. Ali, "Design of bandpass filter for 5G applications with high-selectivity and wide band rejection," in *2022 Muthanna International Conference on Engineering Science and Technology (MICEST)*, 179–183, Samawah, Iraq, Mar. 2022.
- [5] Yang, H.-C. and M.-S. Alouini, *Advanced Wireless Transmission Technologies: Analysis and Design*, Cambridge University Press, 2020.
- [6] Weng, M.-H., S.-W. Lan, S.-J. Chang, and R.-Y. Yang, "Design of dual-band bandpass filter with simultaneous narrow-and wide-bandwidth and a wide stopband," *IEEE Access*, Vol. 7, 147 694–147 703, 2019.
- [7] Wei, F., J. H. Yu, C. Y. Zhang, C. Zeng, and X. W. Shi, "Compact balanced dual-band BPFs based on short and open stub loaded resonators with wide common-mode suppression," *IEEE Transactions on Circuits and Systems II: Express Briefs*, Vol. 67, No. 12, 3043–3047, Dec. 2020.
- [8] Tang, J., H. Liu, and Y. Yang, "Compact wide-stopband dual-band balanced filter using an electromagnetically coupled SIR pair with controllable transmission zeros and bandwidths," *IEEE Transactions on Circuits and Systems II: Express Briefs*, Vol. 67, No. 11, 2357–2361, Nov. 2020.
- [9] Sajadi, A., A. Sheikhi, and A. Abdipour, "Analysis, simulation, and implementation of dual-band filtering power divider based on terminated coupled lines," *IEEE Transactions on Circuits and Systems II: Express Briefs*, Vol. 67, No. 11, 2487–2491, Nov. 2020.
- [10] Belmajdoub, A., M. Jorio, S. Bennani, A. Lakhssassi, and M. Amzi, "Design of compact microstrip bandpass filter using square DMS slots for Wi-Fi and bluetooth applications," *TELKOMNIKA (Telecommunication Computing Electronics and Control)*, Vol. 19, No. 3, 724–729, Jun. 2021.
- [11] Wang, X., Y. Li, H. Li, Z.-Y. Zong, and W. Wu, "Compact single- and dual-band band-pass filters employing mixed eighth-mode substrate-integrated waveguide and microstrip line resonators," *IET Microwaves, Antennas & Propagation*, Vol. 17, No. 3, 190–199, Feb. 2023.
- [12] Li, S., S. Li, J. Yuan, J. Liu, and M. Shi, "Fully tunable band-pass filter with wide bandwidth tuning range and switchable single/dual band," *IEEE Access*, Vol. 12, 36 577–36 585, 2024.

- [13] Alqaisy, M., C. K. Chakrabraty, J. K. Ali, A. R. Alhawari, and T. Saeidi, "Switchable square ring bandpass to bandstop filter for ultra-wideband applications," *International Journal of Microwave and Wireless Technologies*, Vol. 9, No. 1, 51–60, 2017.
- [14] Arain, S., P. Vryonides, K. Nisar, A. Quddious, and S. Nikolaou, "Novel selective feeding scheme integrated with SPDT switches for a reconfigurable bandpass-to-bandstop filter," *IEEE Access*, Vol. 9, 25 233–25 244, 2021.
- [15] Velgaleti, S. B. and S. Nalluri, "Analysis of a compact dual/single band tunable BPF for 5G/X-band applications," *Progress In Electromagnetics Research M*, Vol. 124, 125–133, 2024.
- [16] Hong, J.-S. G. and M. J. Lancaster, *Microstrip Filters for RF/Microwave Applications*, John Wiley & Sons, 2004.
- [17] Chen, C.-F., H.-Y. Tseng, Y.-H. He, and W.-J. Li, "Design of compact microstrip bandpass filter with two switchable operating passbands," *Electronics Letters*, Vol. 58, No. 1, 19–21, Jan. 2022.
- [18] Fan, M., K. Song, and Y. Fan, "Reconfigurable bandpass filter with wide-range bandwidth and frequency control," *IEEE Transactions on Circuits and Systems II: Express Briefs*, Vol. 68, No. 6, 1758–1762, Jun. 2021.
- [19] Wei, Z., T. Yang, P.-L. Chi, X. Zhang, and R. Xu, "A 10.23–15.7-GHz varactor-tuned microstrip bandpass filter with highly flexible reconfigurability," *IEEE Transactions on Microwave Theory and Techniques*, Vol. 69, No. 10, 4499–4509, Oct. 2021.